JME

Journal of Mining & Environment,
Vol.5, No.1, 2014, 1-12.

Karstic water exploration using the Schlumberger VES and dipole–dipole resistivity profiling surveys in the Tepal area, west of Shahrood, Iran

F. Sharifi[1], A. R. Arab-Amiri[2*], A. Kamkar-Rouhani[3]

1. M.Sc. Student, Faculty of Mining, Petroleum and Geophysics, Shahrood University of Technology
2. Assistant Prof., Faculty of Mining, Petroleum and Geophysics, Shahrood University of Technology
3. Associate Prof., Faculty of Mining, Petroleum and Geophysics, Shahrood University of Technology

Received 15 January 2013; received in revised form 11 April 2014; accepted 23 April 2014
Corresponding author: alirezaarabamiri@yahoo.com (A. R. Arab-Amiri).

Abstract
To have sustainable development in a country, the need for clean groundwater resources is undoubted. Due to the importance and high quality of karstic waters in supplying water in Iran, especially in Shahrood city, this study aim to recognize and explore Karstic waters in southwest of Tepal area, Shahrood. For this purpose, the study used the integration of the results obtained from the methods of vertical electrical sounding (VES) and resistivity profiling. The VES surveys were performed in 10 sounding points using the Schlumberger array with electrode separations of a maximum 500 meters. The resistivity profiling surveys were carried out along four lines with a length of more than four kilometers using dipole-dipole electrode array with 75m electrode spacing and dipole steps 1 to 8 in the study area. Then, one-dimensional (1-D) modeling and interpretation of the sounding results, using master curves and IX1D software, and two-dimensional (2-D) modeling and interpretation of the profiling results using Res2DINV were made. As a result of the interpretation and integration of the results, karstic water zones in the study area were recognized, and based on that, suitable locations for drilling to access and extract karstic groundwater were introduced.

Keywords: *Vertical electrical sounding (VES), Resistivity profiling, Karstic water, Schlumberger array, Dipole-dipole array.*

1. Introduction

Karstic terrains cover approximately 12% of the earth's continental surface and 25% of the world's population is supplied partially or entirely by karstic water resource [1]. Also approximately 11% of Iran territories are covered by carbonate rocks [2] and the study area, along Tepal Mountains, was occupied by exposed karstified carbonate rocks. Due to the importance and high quality of karstic water, this research aims to explore karstic waters in study area.

In hard rock areas, fractured zones are important to be identified and characterized since they lead to preferential groundwater flow pathways and enhance well productivity [3], thus they must be recognized for aquifers exploitation in these areas. Also, information on karstic water resources characteristics provides threshold values for different water base activities. Therefore, due to vital importance of karstic water, attempts for the exploration of new resources of this style are inevitable.

To investigate karstic water resources, various methods have been used by researchers. For example Jaiswal et al. [4], Srinivasa Rao and Jugran [5] and Sener et al. [6] have used surficial evidence only for this purpose, but Srivastava and Bhattacharya [7] have applied surficial evidence and geoelectrical methods, Ravi Shankar and Mohan [8] and Subba Rao [9] have used a combination of surficial and hydrogeological evidence and finally, Israil et al. [10] and Riyadh et al. [11] have employed surficial, hydrogeological and geophysical reconnaissance.

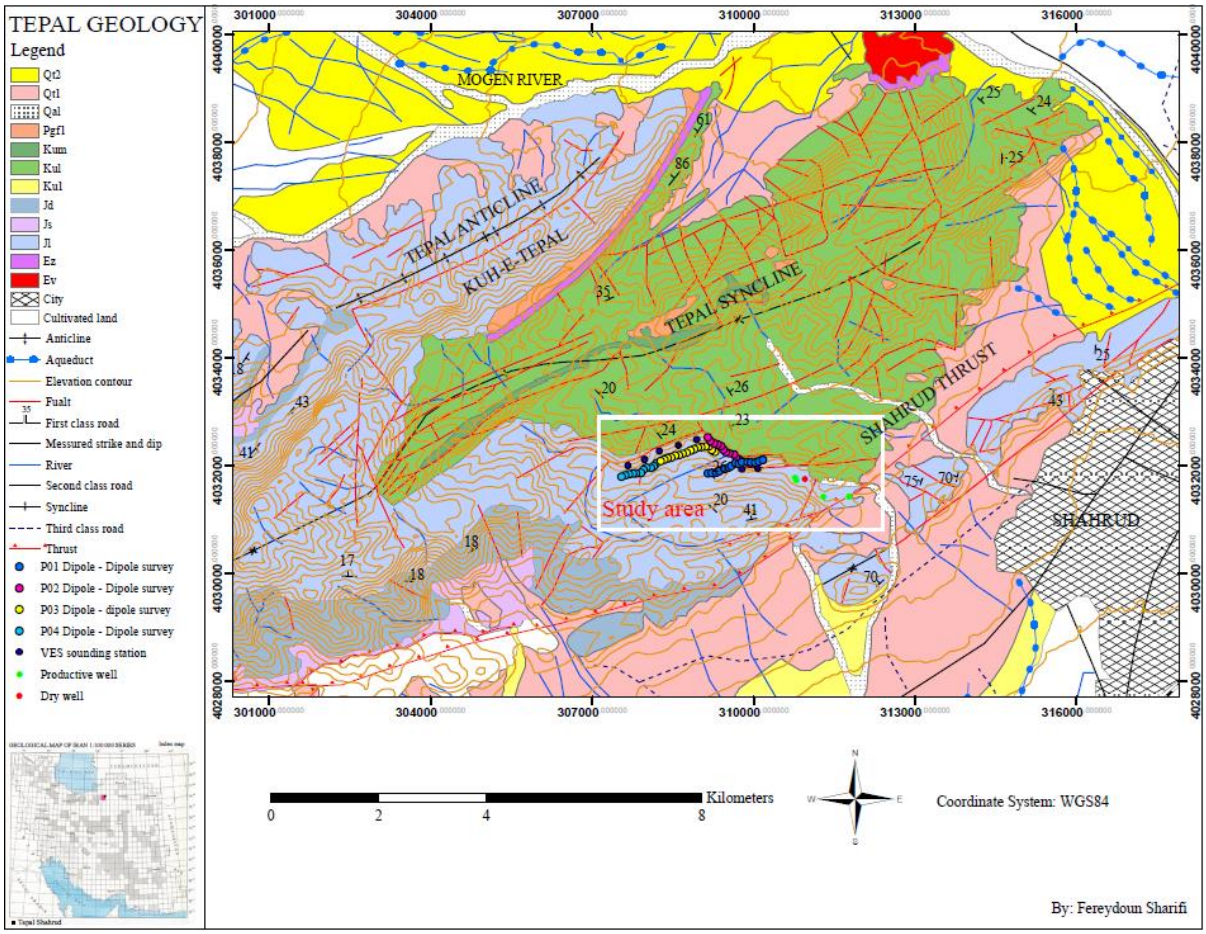

Figure 1. Geological map of the Tepal area (the study area is surrounded by white rectangle) [12].

When geological or hydrogeological information is scarce or missing, non-destructive geophysical exploration is an efficient way to obtain information from the subsurface. For several decades, numerous geophysical studies have been carried out to investigate karstic structures; e.g., Šumanovac and Weisser [13], and Vasconcelos and Grechka [14] and yang et al. [15] have used seismic methods and Noel and Xu [16], Guérin and Benderitter [17], Gautam et al. [18], Kaufmann and Quinif [19], Zhou et al. [20], Gibson et al. [21], Deceuster et al. [22] and Qarqori et al. [23] have applied electrical resistivity imaging (ERI) for hydrogeological or geotechnical purposes, and Jardani et al. [24] and Suski et al. [25] have employed self-potential methods to characterize fractures or karsts. Along the same lines, Robert et al. [26] have used the contribution of electrical resistivity tomography (ERT) and self-potential (SP) methods for a water well drilling program in fractured/karstified limestones.

Magnetic resonance sounding (MRS) allows geophysicists to access water content information directly and then to locate shallow water-filled karst conduits (20-30m depth investigation) [27, 28] or to position high yield extraction wells [29, 30] and localize cavities [31]. Ground penetration radar (GPR) [32, 33, 34] and electromagnetic very low frequency (VLF) [35] have been used successfully to localize cavities, and to estimate the mean azimuth of the fracturing, respectively. Also susceptibility models have been used to investigate karst and sinkholes in several cases [36-38].

Alternatively applied conventional methods for karstic water exploration are as follows:

a. Regional scale; by combining surficial evidence such as geology, precipitation, fractures concentration, topography and drainage network with hydrogeological evidence such as groundwater table and charge of the springs.
b. Local scale; usually appropriate ground-based geophysical surveys are carried out.

Non-uniqueness of geophysical interpretation, due to inversion or inherent geological ambiguities, may require the use of several methods to reduce the uncertainty [39-43]. In this regard Qader Aziz and Mohammad Ali [44] have combined surveys using Ground Penetrating Radar and Electrical Resistivity Tomography to provide a cost-effective characterization of the subsurface karst environments. A modern approach to understand the implications of the geometry, distribution and status of the fracture network in water circulation should be based on a detailed study of the geology of the area. Geology represents the basis for the effective study and management of water resources. Our investigation includes the results of comprehensive geology and geophysical survey conducted in the Tepal area, Shahrood (Figure 1). The layout map of the study area, which includes lithological units, fractures, drainage and elevation contours are delineated In Figure 1.

DC resistivity survey is an efficient tool for characterizing fractured or karstic zones due to the contrast in electrical resistivity [45, 46, 47], but can encounter problems when exploring greater depths [13, 27, 29].

In this study, the Schlumberger VES and dipole-dipole electrical resistivity profiling surveys were carried out in July 2011 using Swedish ABEM Company resistivity meter (Terrameter SAS-4000) to explore karstic water zones in the study area. Based on the results, suitable locations for drilling to access and extract karstic ground water have been introduced.

2. Geological outline and local setting

Shahrood city is located in the north-east of Iran, and its geological setting represents eastern Alborz zone. The Alborz Mountains are a continuation of the Alpine type Mountains, which are a complex asymmetric belt of folded and faulted rocks [48]. Tepal Mountains, as shown in Figure 1, are situated in the west to north-west of Shahrood city. In this area, the influence of folding and high intense fault system, crushed zone and secondary porosity have prepared appropriate conditions for developing karstic aquifer formation.

According to the geological map of Tepal area (Figure 1), the study area is located in the middle to upper Jurassic Lar formation (Jl), characterized by light grey, thick bedded to massive limestone and cherty limestone, ammonite bearing with absence of marl sequences [12].

In the study area five wells have been drilled. The locations of these five wells in the study area are presented by symbols A, B, C, D and E in Figure 2. The well A has been drilled on the Shahrood thrust. There are also numerous dissolved cavities around other wells as a surficial evidence of karstification occurrence. Well C (red point), is a dry well, but other wells are productive as groundwater is currently extracted from these wells. Also in Figure 2, the positions of geo-electrical surveying points and lines, composed of the Schlumberger VES points and dipole-dipole profiling lines, are presented.

3. Geophysical surveys

Two basic types of field procedure are in common use for electrical resistivity surveys: vertical electrical sounding (VES) and electrical resistivity profiling. In resistivity sounding, the electrode spacing interval is changed while maintaining a fixed location for the center of the electrode spread; consequentially in a general way as the electrode spacing increases the depth of investigation increases [49]. The interpretation result of a resistivity sounding dataset is demonstrated in one-dimensional (1-D) form that includes resistivities and thicknesses of the subsurface layers. To interpret the data from such a survey, it is normally assumed that the subsurface consists of horizontal layers and it does not take into account lateral changes in the layer resistivity. The failure to include the effect of such lateral changes can result in errors in the interpreted layer resistivity and/or thickness [50].

In resistivity profiling, the location of the spread is changed while maintaining a fixed electrode spacing interval and entire array is moved along a straight line. This gives some information about lateral changes in subsurface resistivity related to each median depth of investigation. In this case, it is assumed that resistivity does not change in the direction that is perpendicular to the survey line. The interpretation result of a resistivity profiling dataset can be demonstrated in 1-D or two-dimensional (2-D) forms. In the latter case, the resistivity profiling should have been carried out along several lines by employing an electrode spacing or along a line using multiple electrode spacings.

In general, linear electrode configurations are used for resistivity profiling measurements. Common configurations are the Schlumberger, Wenner and dipole-dipole spreads [51]. Some factors affecting the choice of array type are explained in Table 2. The dipole-dipole array is very sensitive to horizontal changes in resistivity, but relatively insensitive to vertical changes in the resistivity. That means that it is good in mapping vertical structures, such dykes and cavities, but relatively poor in mapping horizontal structures such as sills or sedimentary layers. The median depth of investigation of this array depends on both the dipole spacing and the dipole step or dipole separation factor that are normally defined by "a" and "n" symbols, respectively [50]. In this array, as the dipole separation factor "n" increases, the depth of investigation increases.

In the electrical resistivity method, one can expect that water-bearing fractured zones have contrast strongly with compact bedrock. These are good targets for electrical resistivity investigation. In the study area due to the existence of bedding with a low dip (see Figure 1), the deep water table (Table 1) can be detected by performing VES surveys using Schlumberger array. Because of the presence of essential inhomogeneities in such karstified areas, it is normally required to use several methods for obtaining enough information from the subsurface ground. Due to low sensitivity of the Schlumberger array to lateral inhomogeneities, and also good characteristics of the dipole-dipole array, especially its moderate depth of penetration, low EM coupling between the current and potential circuits and high sensitivity to horizontal changes in resistivity, the combination of these two arrays for vertical electrical sounding and electrical resistivity profiling, respectively, can lead to an optimized resistivity survey method in the study area.

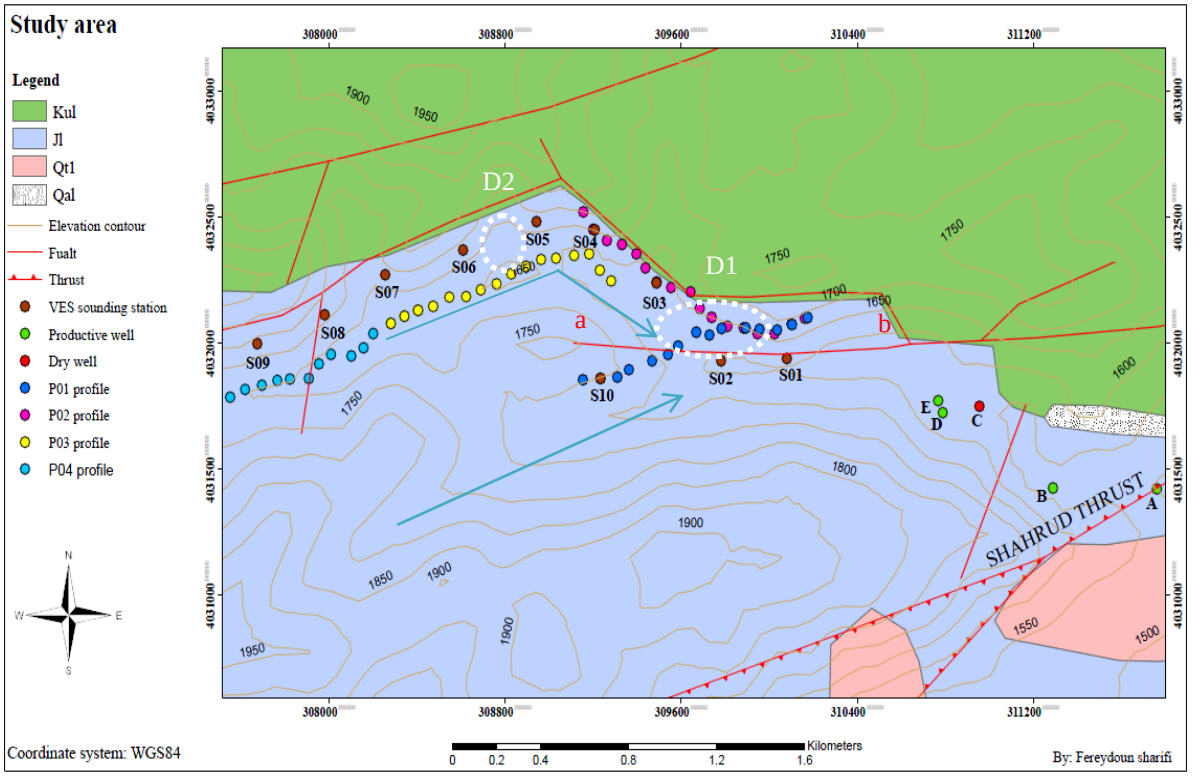

Figure 2. The geological map superimposed on topographical contour map of the study area, in which the locations of 10 resistivity sounding points S01 to S10 and 4 lines denoted by different color dots are also demonstrated.

Table 1. The existing well information in the study area

Well ID.	A	B	C	D	E
Water table (m)	-	-	dry	150	165
Well depth (m)	120	160	-	300	280

Table 2. Comparison of the Wenner, Schlumberger and dipole-dipole electrode arrays [53].

Criteria	Wenner	Schlumberger	Dipole - Dipole
Vertical resolution	Good	Moderate	Poor
Depth of penetration	Poor	Moderate	Good
Suitability to VES	moderate	Good	Poor
Sensitivity to orientation	Yes	Yes	Moderate
Sensitivity to lateral inhomogeneities	High	Moderate	Moderate
Labor intensive	Yes(no*)	Moderate(no*)	Moderate(no*)
Availability of interpretational aids	Good	Good	Moderate

***when using a multicore cable and automated electrode array

4. Discussions on the results obtained

According to Parizek [52], the most portion mainstream (60-80%) in carbonate areas is controlled by solution process and weathering along fractures. The wells drilled along mainstream intersect more porous and intensively weathered rocks in respect to the wells drilled at high elevations in the same hard rock. Thus for this reason and because of relatively low to moderate topography conditions (Figure 2) in the study area, the geoelectrical surveys were carried out along the mainstream bed.

The VES surveys have been carried out in 10 resistivity sounding points S01 to S10 (Figure 2) using the Schlumberger array with electrode separations of maximum 500 meters. In addition, the resistivity profiling surveys were carried out along 4 lines (Figure 2) of more than 4 kilometers long using dipole-dipole electrode array with 75m electrode spacing and dipole steps 1 to 8 in the study area.

The measured data by using the Schlumberger and dipole-dipole arrays are converted to apparent resistivity by applying equation (1) and (2), respectively.

$$\rho_a = \frac{\pi c^2}{b}[1-\frac{b^2}{4c^2}]R; \quad c \geq 5b \tag{1}$$

$$\rho_a = \pi n(n+1)(n+2)aR \tag{2}$$

where ρ_a, R, a, b, c and n represent the apparent resistivity, measured resistance, dipole spacing, potential electrode spacing, half of current electrode spacing and dipole step, respectively [53].

1-D modeling and interpretation of the VES data using theoretical master curves and IX1D software (produced by Interpex Company), and 2-D modeling and interpretation of the resistivity profiling data using RES2DINV were made. The resistivity modeling and interpretation results of the VES and resistivity profiling data are given in Figures 3 and 4, and Tables 3 and 4.

Based on the VES curves indicated in Figure 3 and the interpretation results indicated in Table 3, we can summarize the interpretation results of all sounding points as illustrated in Table 4.

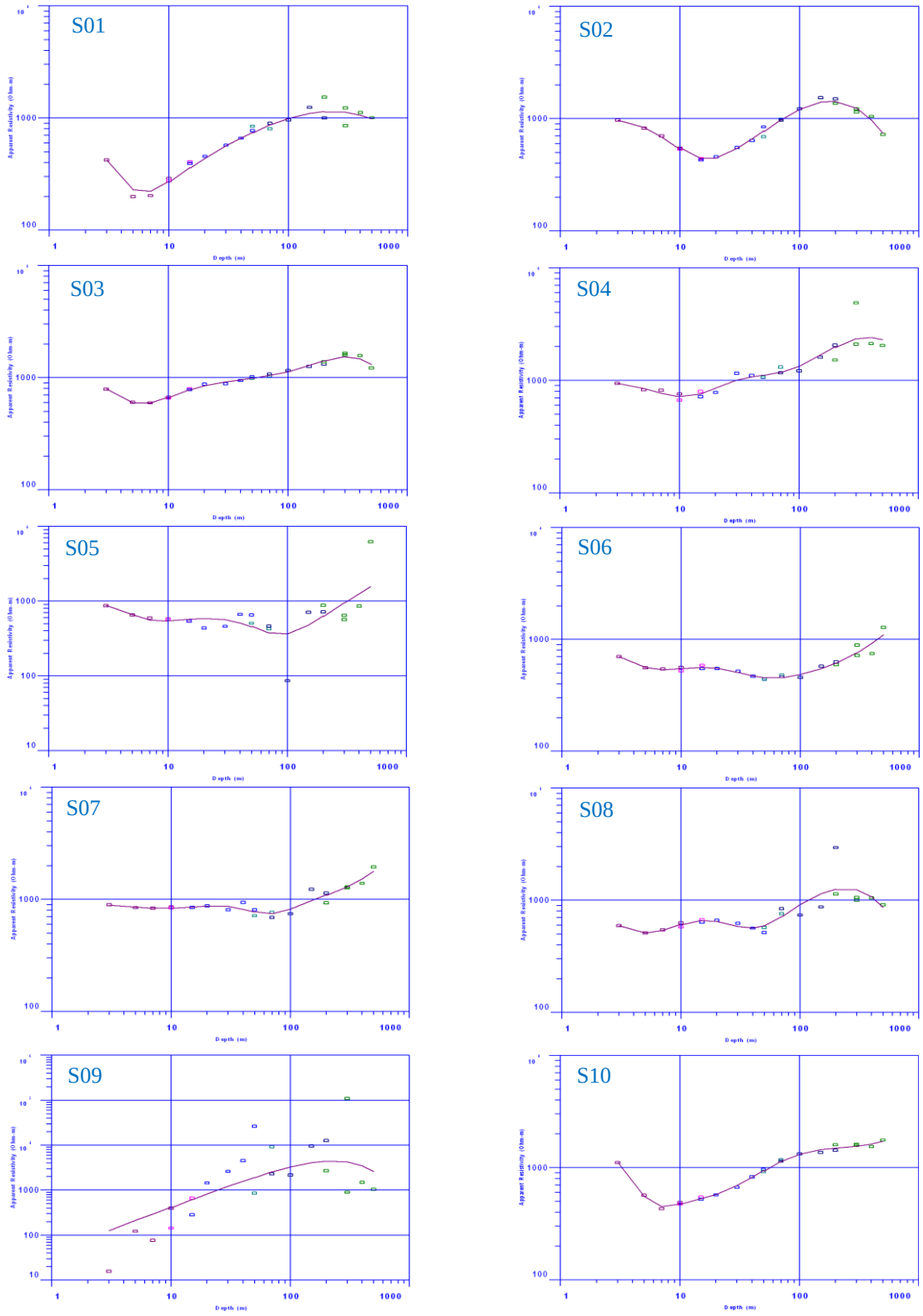

Figure 3. 1-D modeling and interpretation results of the VES S01-S10, obtained using IX1D software

Table 3. Corresponding interpretation of VES S01 - S10 (Resistivity (R) and geoelectrical layer thickness (T) values are in ohm-meter and meter, respectively).

ID.	S01		S02		S03		S04		S05		S06	
RMS	12.31%		4.77%		3.5%		19.85%		62.89%		7.48%	
N	R	T	R	T	R	T	R	T	R	T	R	T
1	902.42	1.12	1028.1	3.39	1099.3	1.47	985	2.49	1057.5	2.16	939.09	1.33
2	255.32	0.19	315.16	11.62	325.18	2.49	753.07	1.76	203.23	1.29	408.51	2.58
3	123.62	2.56	818.62	10.25	1647.9	3.18	327.57	2.65	706.19	18.41	693.82	9.23
4	290.08	2.00	3834.6	67.83	857.86	7.05	693.97	2.13	789.59	3.32	338.92	26.14
5	971.17	15.49	275.64	∞	932.47	11.71	2797.4	9.81	94.252	17.96	601.89	170.25
6	14422.1	30.60	****	****	1489.3	16.17	437.16	18.28	152.57	5.63	5369.1	∞
7	775.69	7.48	****	****	637.35	21.92	1379.8	14.51	443.13	14.95	****	****
8	1575.4	91.64	****	****	1238.4	15.31	13554	52.31	1299.9	15.59	****	****
9	729.45	∞	****	****	3442.6	25.65	5076.1	51.33	0.1242E	∞	****	****
10	****	****	****	****	5563.4	71.60	233.94	∞	****	****	****	****
11	****	****	****	****	97.956	∞	****	****	****	****	****	****

Table 3. Continued.

ID.	S07		S08		S09		S10	
RMS	8.46%		23.62%		260.64%		3.25%	
N	**R**	**T**	**R**	**T**	**R**	**T**	**R**	**T**
1	915.31	1.99	738.51	1.67	10.06	0.22	2065.3	1.23
2	782.77	9.08	196.5	1.38	1385.4	0.70	1427.8	0.21
3	2231.4	5.92	1668.7	5.06	440.14	0.21	220.96	2.12
4	200.07	12.40	165.61	12.02	58468	24.95	846.08	4.22
5	521.17	5.60	8010.1	39.11	345.93	252.98	308.76	7.01
6	4700.7	19.29	757.86	3.69	91089	26.68	3337	32.81
7	909.16	151.68	501.69	42.80	0.22E	∞	878.29	35.01
8	725.39	10.56	118.34	∞	****	****	1442.6	159.25
9	29360	∞	****	****	****	****	2842.7	****
10	****	****	****	****	****	****	****	****
11	****	****	****	****	****	****	****	****

Table 4. Interpretation of VES surveys in sounding locations or points S01 to S10

Point	Interpretation
S01	Represents 9 high resistive geoelectrical layers.
S02	In the depth of more than 93 m, the resistivity decreases to 275 Ω.m which can indicate a poor to moderate potential of karstic water resource.
S03	In the depth of more than 176 m, the low resistivity layer (98 Ω.m) can be related to a moderate to good potential of karstic water resource.
S04	In the depth of more than 155 m, a geoelectrical layer with a resistivity of 233 Ω.m shows a poor potential of water resource.
S05	In the depth of 25-48 m, a moderate potential of water source can be estimated.
S06	Resistivities of the subsurface layers are higher than the resistivity value water-bearing formations, and thus, no water-bearing zone is found.
S07	Resistivities of the subsurface layers are higher than the resistivity value water-bearing formations, and thus, no water-bearing zone is found.
S08	Possible existence of a water-bearing zone with a resistivity of 118 Ω.m in the depth of more than 105 m.
S09	Absence of water-bearing zone
S10	Absence of water-bearing zone

The inversion modeling results of the resistivity profiling data along 4 lines P01, P02, P03 and P04, represented by resistivity sections in Figure 4, imply various resistive and conductive zones in the subsurface. The conductive zones illustrated by white dashed areas in the resistivity sections P01, P02 and P03 represent favorite karstic water zones.

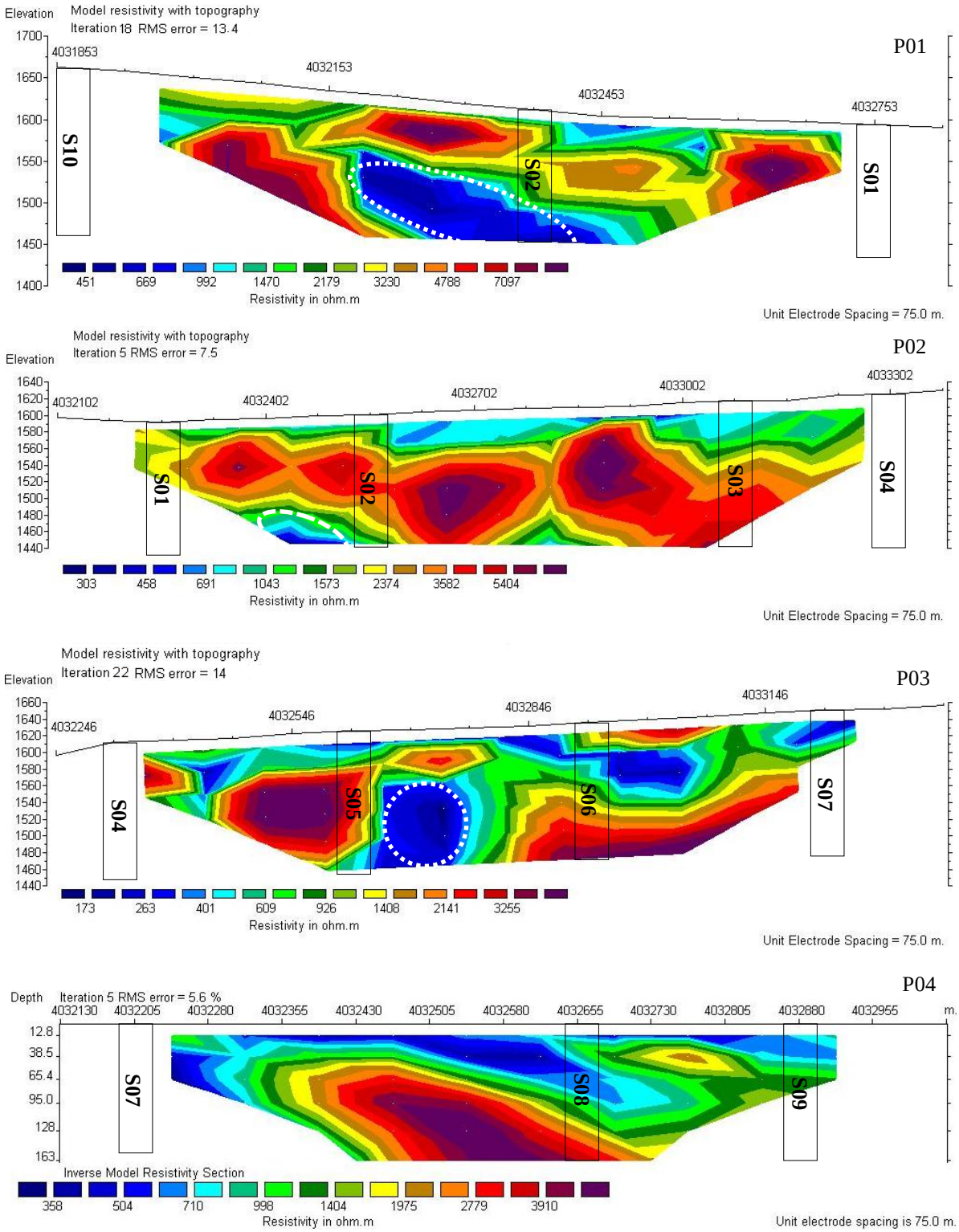

Figure 4. The 2-D modeling and interpretation results of the resistivity profiling data along 4 lines P01, P02, P03 and P04, obtained using RES2DINV Software. The VES locations or points S01 to S10 across these resistivity profiling sections are also shown.

5. Conclusions

Lithology, precipitation, low dip bedding and faulted zone are the favorite criteria, which control karstification. The geological map of the study area (Figures 1 and 2), that illustrates limestone formations without of marl sequences, implies favorite lithological and tectonic conditions for karstification and occurrence of karstic water in the subsurface. Similarly, the mean annual rainfall of 130 mm in the Shahrood region, and the presence of low dip bedding and faulting systems in the limestone formations, provides favorite conditions in the study area, where secondary porosity could be formed. Therefore, the existence of water-bearing zones in the subsurface can be expected. The presence of productive water wells in the area (Figure 2) is also another strong reason for prospecting and finding new karstic groundwater in the area.

This stuy has been conducted to explore karstic water in the southwest of Tepal area, north to northwest of Shahrood. To this end, electrical resistivity methods comprising of VES (using Schlumberger array) and resistivity profiling (using dipole-dipole array) were carried out in the area, and then, the measured results were modeled and interpreted.

Fault ab, shown in Figure 2, that intersects P01 resistivity profiling section, creates a crushed zone with a low resistivity (the area which surrounded by the white dashed line in Figure 4) which its dip direction is towards the north. The intersection point of ab fault and two mainstreams in study area, presented with light blue arrow in the geological map of Figure 2, can be considered as the evidence of subsurface solution development. Also, the VES results in sounding point S02, and the resistivity profiling sections along P01 and P02 lines confirm aforementioned conclusion. Consequently, white-dashed line ellipse in the resistivity section along P01 and white circular dashed line in the resistivity section along P03 are proposed as the first and second priority for drilling to access karstic groundwater (Figure 2).

Acknowledgements

Authors wish to thank Dr. M. H. Loke for his guidance in modeling resistivity data by RES2DINV software, Mr. Mehdi Zarei, the head of Shahrood University of Technology Geophysical Laboratory for his assistance in geophysical surveying and use of the Laboratory facilities, Mr. Seyed Ali Hossinizadeh and Mr. Ali Akbar Frootan for their assistance in geophysical surveying, Water Administration and Dispatching Company of Shahrood city for their financial support and permission to use the required information.

References

[1]. Ford, D. and Williams, p. (2007). Karst Hydrogeology and Geomorphology, John Wiley & son Ltd, England, pp. 1-562.

[2]. Afrasiabian, A. (1998). Importance of study and research on karst water resources on Iran, proceeding on the 2nd international symposium on karst water resources, Tehran, Kermanshah, Iran, pp.126-137.

[3]. Berkowitz, B. (2002). Characterizing flow and transport in fractured geological media: a review, Advances in water Resources, 25:861-884.

[4]. Jaiswal, R.K., Mukherjee, S., Krishnamurthy, J. and Saxena, R. (2003). Role of remote sensing and GIS techniques for generation of groundwater prospect zones towards rural development - an approach, International Journal of Remote Sensing, 24:993 – 1008.

[5]. Srinivasa Rao, Y. and Jugran, D. K. (2003). Delineation of groundwater potential zones and zones of groundwater quality suitable for domestic purposes using remote sensing and GIS, Hydrological Sciences Journal, 48:821- 833.

[6]. Sener, E., Davraz, A. and Ozcelik, M. (2005). An integration of GIS and remote sensing in groundwater investigations: A case study in Burdur, Turkey, Hydrogeology Journal, 13:826-834.

[7]. Srivastava, P.K. and Bhatacharya, A. (2006). Groundwater assessment through an integrated approach using remote sensing, GIS and resistivity techniques: a case study from a hard rock terrain, International Journal of Remote Sensing, 27:4599 – 4620.

[8]. Ravi Shankar, M.N. and Mohan, G. (2006). Assessment of the groundwater potential and quality in Bhatsa and Kalu river basins of Thane district, western Deccan Volcanic Province of India, Journal of Environmental Geology, 49:990-998.

[9]. Subba Rao, N. (2006). Groundwater potential index in a crystalline terrain using remote sensing data", Journal of Environmental Geology, 50:1067-1076.

[10]. Israil, M., Al-hadithi, M. and Singhal, D.C. (2006). Application of a resistivity survey and geographical information system (GIS) analysis for hydrogeological zoning of a piedmont area, Himalayan foothill region, India, Hydrogeology Journal, 14:753-759.

[11]. Riyadh, R.Y., Ros Fatihah, M., Samsudin, H.T. (2013). Integrated Techniques To Identify Consequences Of Sinkhole Hazards For Constructing Housing Complexes On Carbonate Karst Terrains In Perak, Peninsular Malaysia", International Journal of Engineering Research & Technology (IJERT), 2(7):2292-2328.

[12]. Vaziri, S.H., Majidifard, M.R. and Saidi, A. (2001). Geological map of Iran 1:100,000 sheet No. 6962, geological survey of Iran.

[13]. Šumanovac, F. and Weisser, M. (2001). Evaluation of resistivity and seismic methods for hydrogeological mapping in karsts terrains, Journal of Applied Geophysics, 47:13-28.

[14]. Vasconcelos, I. and Grechka, V. (2007). Seismic characterization of multiple fracture sets at Rulison Field, Colorado, Geophysics, 72: B19-B30.

[15]. Yang, Y-S., Li, Y-Y., Cui, D-H. (2013). Identification of karst features with spectral analysis on the seismic reflection data, Environmental Earth Sciences, Springer-Verlag Berlin Heidelberg, doi.10.1007/s12665-013-2477-x.

[16]. Noel, M. and Xu, B. (1992). Cave detection using Electrical Resistivity Tomography (ERT)", Cave science 19 pp. 91-94.

[17]. Guérin, R. and Benderitter, Y. (1995). Shallow karst exploration using MT-VLF and DC resistivity methods, Geophysical prospecting, 43:635- 653.

[18]. Gautam, P., Pant, S.R. and Ando, H. (2000). Mapping of subsurface karst structure with gamma ray and electrical resistivity profiles: a case study from pokharavally, centeral Nepal, journal of Applied Geophysics 45:97-110.

[19]. Kaufmann, O. and Quinif, Y. (2002). Geohazard map of cover-collapse sinkholes in the Tournaisis area, southern Belgium", Engineering geology, 65:117-124.

[20]. Zhou, W., Beck, B.F. and Adams, A.L. (2002). Effective electrode array in mapping karst hazards in electrical resistivity tomography, Environmental geology, 42:922-928.

[21]. Gibson, P.J., Lyle, p. and George, D.M. (2004). Application of resistivity and magnetometry geophysical techniques for near-surface investigations in Karstic terrains in Irland, Journal of cave and karst Studies, 66:35-38.

[22]. Deceuster, J., Delgranche, J. and Kaufmann, O. (2006). 2D cross-borehole resistivity tomographies below foundations as a tool to design proper remedial actions in covered karst, Journal of Applied Geophysics, 60:68-86.

[23]. Qarqori, K.h., Rouai, M., Moreau, F., Saracco, G., Dauteuil, O., Hermitte, D., Boualoul, M. and Le Carlier de Veslud, C. (2012). Geoelectrical Tomography Investigating and Modeling of Fractures Network around Bittit Spring (Middle Atlas, Morocco)", International Journal of Geophysics, 2012, 13p. doi.org/10.1155/2012/489634.

[24]. Jardani, A, Dupont, J.P. and Revil, A. (2006a). Self-potential signals associated with preferential groundwater flow pathways in sinkholes, journal of Geophysical Research, 111:1-13.

[25]. Suski, B., Lander, F., Baron, L., Vuataz, F.D., Philippossian, F. and Holliger, K. (2008). Detection and characterization of hydraulically active fractures in carbonate aquifer: results from self-potential, temperature and fluid electrical conductivity logging in the Combioula hydrothermal system in the southwestern Swiss Alps, Hydrogeology Journal, 16:1319-1328.

[26]. Robert, T., Dassargues, A., Brouyère, S., Kaufmann, O., Hallet, V., Nguyen, F. (2011). Assessing the contribution of electrical resistivity tomography (ERT) and self-potential (SP) methods for a water well drilling program in fractured/karstified limestones, Journal of Applied Geophysics, 75:42–53.

[27]. Boucher, M., Girard, J.F., Legchenko, A., Baltassat, J.M., DÖrfliger, N. and Chalikakis, K. (2006). Using 2D inversion of magnetic resonance soundings to locate a water-filled karst conduit, Journal of Hydrogeology, 330:413-421.

[28]. Legtchenko, A. (2013). Magnetic Resonance Imaging for Groundwater, Wiley-ISTE, 235 p.

[29]. Vouillamoz, J.M., Descloitres, M., Bernard, J., Fourcassier, P. and Romagny, L. (2002). Application of integrated magnetic resonance sounding and resistivity methods for borehole implementation. A Case Study in Cambodia, Journal of Applied Geophysics, 50:67-81.

[30]. perttu, N., person, L., ErlstrÖm, M. and Elming S., (2012). Magnetic resonance sounding and radiomagnetotelluric measurements used to characterize a limestone aquifer in Gotland, Sweden, Journal of Hydrology, 424-425:184-195. doi.org/10.1016/j.jhydrol.2011.12.042.

[31]. Vouillamoz, J.M., Legchenko, A., Albouy, Y., Bakalowicz, M., Baltassat, J.M. and Al-Fares, W. (2003). Localization of karst aquifer with magnetic resonance sounding and resistivity imagery, Ground-water, 41:578-586.

[32]. Al-Fares, W., Bakalowicz, M., Guérin, R. and Dukhan, M. (2002). Analysis of the karst aquifer structure of the Lamalou area (Hérault, France) with ground penetrating radar, Journal of Applied geophysics, 51:97-106.

[33]. Marcak, H., Golebiowski, T., Tomecka-Suchon, S. (2008). Geotechnical analysis and 4D GPR measurements for the assessment of the risk of

sinkholes occurring in a Polish mining area, Near Surface Geophysics, 6(4):233–243.

[34]. Carrière, S.D., Chalikakis, K., Sénéchal, G., Danquigny, C., Emblanch, C. (2013). Combining Electrical Resistivity Tomography and Ground Penetrating Radar to study geological structuring of karst Unsaturated Zone, Journal of Applied Geophysics, 94:31–41.

[35]. Bosch, F.P. and Müller, I. (2001). Continuous gradient VLF measurements: a new possibility for high resolution mapping of karst structures, First Break 19:343-350.

[36]. Galve, J.P., Bonachea, J., Remondo, J., Gutierrez, F., Guerrero, J., Lucha, P., Cendrero, A., Gutierrez, M. and Sanchez, J.A. (2008). Development and validation of sinkhole susceptibility models in mantled karst settings. A case study from the Ebro valley evaporite karst (NE Spain), Eng Geol., 99:185–197.

[37]. Garcia-Moreno, I., Mateos, R.M. (2011). Sinkholes related to discontinuous pumping: susceptibility mapping based on geophysical studies. The case of Crestatx (Majorca, Spain), Environ Earth Sci., 64:523–537.

[38]. Margiotta, S., Negri, S., Parise, M., Valloni, R. (2012). Mapping the susceptibility to sinkholes in coastal areas, based on stratigraphy, geomorphology and geophysics", Natural Hazards, 62:657–676. doi 10.1007/s11069-012-0100-1.

[39]. Bernard, J. and Valla, P. (1991), Groundwater exploration in fissured media with electrical and VLF method, Geo exploration, 27:81-91.

[40]. Krishnamurthy, N.S., Kumar, D., Ananda Rao, V., Jain, S.C. and Ahmed, S. (2003). comparison of surface and sub-surface geophysical investigation in delineating fracture zones, Current Science 84:1242-1246.

[41]. Porsani, J.L., Elis, V.R. and Hiodo, F.Y. (2005). Geophysical investigations for the characterization of fractured rock aquifers in Itu, SE Brazil, Journal of Applied Geophysics, 57:119-128.

[42]. Delle Rose, M., Leucci, G. (2010). Towards an integrated approach for characterization of sinkhole hazards in urban environments: the unstable coastal site of Casalabate, Lecce, Italy, Journal of Geophysics and Engineering, 7:143–154.

[43]. Kaufmann, G., Romanov, D., Nielbock, R. (2011). Cave detection using multiple geophysical methods: Unicorn cave, Harz Mountains, Germany, Geophysics, 76(3):B71–B77.

[44]. Qader Aziz, B. and Mohammad Ali, P. (2013). Karst cavity detection in carbonate rocks by integration of high resolution geophysical methods, Journal of Zankoy Sulaimani- Part A (JZS-A), 15 (1):159-171.

[45]. Nguyen, F., Garambois, S., Chardon, D., Hermitte, D., Bellier, O. and Jongmans, D. (2007). Subsurface electrical imaging of anisotropic formations affected by a slow active revers fault , Provence, France, Journal of Applied Geophysics, 62:338-353.

[46]. Skinner, D. and Heinson, G. (2004). A comparison of electrical and electromagnetic methods for the detection of hydraulic pathways in a fractured rock aquifer, Clare valley, South Australia", Hydrogeology Journal, 12:576-590.

[47]. Cardarelli, E., Cercato, M., Cerreto, A., Di Filippo, G. (2010). Electrical resistivity and seismic refraction

tomography to detect buried cavities, Geophysical Prospecting, 58:685–695.

[48]. Stoklin, J. (1974). Northern Iran: Alborz Mountains, Mesozoic-Cenozoic Orogenic Belt, Data for Orogenic Studies: Geological Society London. 1st Edn., Scottish Academic Press, London, pp. 213-234.

[49]. Mooney, H.M. (1980). Handbook of Engineering Geophysics: Vol. 2: Electrical Resistivity, Bison Instruments, Inc., 81p.

[50]. Loke, M.H. (2004). Tutorial: 2-D and 3-D electrical imaging surveys, 128 p.

[51]. Kirsch, R. (2006), Groundwater Geophysics-a Tool for Hydrogeology, Springer-Verlag Berlin Heidelberg, pp. 85-116.

[52]. Parizek, R.P., (1976). On the nature and significance of fracture traces and lineaments in carbonate and other terrains", In: Yevejevich, V. karst hydrology and water resources, Water resources publications, Colorado, USA, 1:47-100.

[53]. Reynolds, J.M. (1997). An Introduction to Applied and Environmental Geophysics. pp. 418-459.